Coupling of ultrathin InAs layers as a tool for band-offset determination

J. Brübach,* A. Yu. Silov, J. E. M. Haverkort, W. v. d. Vleuten, and J. H. Wolter
COBRA Interuniversity Research Institute, Eindhoven University of Technology, Department of Physics,
P.O. Box 513, 5600 MB Eindhoven, The Netherlands
(Received 15 July 1998)

We have experimentally determined the band offsets at a highly strained InAs/GaAs interface by means of coupling between two ultrathin InAs layers embedded in a GaAs matrix. When both InAs layers are separated by a 32-ML barrier, the confined electron and light-hole (lh) states are split into symmetric and antisymmetric states, whereas the heavy-hole (hh) level is not split yet. Consequently, the splitting between the hh exciton transitions, which is measured by photoluminescence excitation spectroscopy, is solely determined by the conduction-band offset ΔE_c. Knowing ΔE_c, the hh and lh band offsets ΔE_{hh} and ΔE_{lh} were subsequently determined from the coupling-induced shift and splitting in samples with 16-, 8-, and 4-ML barriers. We find a conduction-band offset of 535 meV, a conduction-band offset ratio of $Q_c=0.58$, and a strain-induced splitting between the hh and lh levels of 160 meV. This method for the direct determination of band offsets is explicitly sensitive to the band-offset ratio, and its application is not restricted to particular type-I semiconductor heterostructures as long as the effective-mass–band-offset product for the conduction and valence bands differs by at least a factor of 2. [S0163-1829(99)01715-4]

I. INTRODUCTION

The optical and electronic properties of ultrathin InAs layers embedded in a GaAs matrix have recently attracted strong interest. This is, on the one hand, due to their potential application in optoelectronic devices.[1,2] On the other hand, since InAs and GaAs have one of the largest lattice mismatches among III-V semiconductors, ultrathin InAs/GaAs quantum wells serve as a model system to study the electronic structure and optical properties in an almost ideal two-dimensional but highly compressively strained material system. In particular, the band alignment, the magnitude of the band offsets, and the degree of confinement are recent topics of intense debate.[3–9]

Within the concept of band offsets, the InAs/GaAs system provides a unique situation. Generally, band offsets are defined for the interface of two semi-infinitely extended layers of material, and for lattice-matched semiconductors this can be realized by means of very wide ''quantum-well'' structures, where size quantization effects become negligible. For the InAs/GaAs system, however, the situation is different. Due to the large lattice mismatch, the critical layer thickness, up to which the growth remains pseudomorphic, amounts only to 2–3 ML.[10] Beyond this critical layer thickness, dislocations are incorporated which in turn may alter the band alignment at the interface,[7] or the formation of self-assembled quantum dots starts to dominate the growth process.[11] As a consequence, ultrathin InAs layers in a GaAs matrix seem to represent the only possibility to access the band offsets at the InAs/GaAs heterointerface at all.

The insertion of an InAs monolayer in a GaAs matrix produces a confining potential on the length scale of the lattice constant, which introduces bound electron, heavy-hole (hh), and light-hole (lh) states in the GaAs band gap, and which in turn give rise to the formation of hh and lh excitons.[12] Due to the large lattice mismatch between InAs and GaAs, the InAs layer is highly compressively strained. As a consequence, the fundamental band gap of the InAs is increased by the hydrostatic strain component, and the shear strain component leads to a splitting between the hh and lh valence bands.[13,14]

In previous papers about the determination of band offsets in InAs/GaAs, the electronic structure of ultrathin InAs layers was described by a quantum-well model.[3,4,6,15–17] Even for monolayer and submonolayer coverages, the potential width is identified as the average InAs layer thickness, and the depth of the confining potential for the electrons or holes as the conduction- or valence-band offsets, which are thus consistently used in the sense of bulk parameters. Furthermore, in this model strain is considered either explicitly in an eight-band $\mathbf{k}\cdot\mathbf{p}$-type effective-mass theory,[4,17] or implicitly by strain-modified values for the band offsets and a different valence-band offset for the hh and lh subbands.[3,7] The procedure which was subsequently applied to determine the band offsets was to measure the optical transition energies for different InAs layer thickness by photoluminescence (PL) or photoluminescence excitation (PLE) and to match the quantum-well calculations with the measurements by fitting the band offsets. However, for unstrained quantum wells it is already questionable whether this procedure provides reliable values for the band offsets, because the transition energies depend on both the confinement energies of the electrons and of the hh's or lh's, respectively, which in this method cannot be separated. In the case of highly strained layers the situation becomes even more troublesome: due to the strain-induced splitting of the hh and lh subbands one needs to determine three band offsets independently from only two optical transitions. This problem is reflected by the large spreading in the band-offset values reported previously, although the same model and the same effective masses were used.[3–6,12,15–18] In the case of ultrathin InAs layers an additional complication arises, since the observed transitions are excitonic ones and the exciton binding energies depend strongly on the InAs layer thickness.[6,19] Thus, in a determination of the band offsets with the above procedure, one has to correct the measured transition energy by the experimen-

 ©1999 The American Physical Society

tally determined exciton binding energy for each InAs layer thickness, or else the calculations have to incorporate explicitly a model for the InAs layer width dependence of the exciton binding energies.

In this paper we report on an alternative method for a determination of band offsets in ultrathin InAs layers without the complications mentioned above. By employing the coupling between two ultrathin InAs layers embedded in a GaAs matrix, and exploiting the large difference in electron and heavy-hole effective masses, we are able to determine the conduction-band offset ΔE_c and the valence-band offsets ΔE_{hh} and ΔE_{lh}, independently. It is well known that in the case of two coupled quantum wells the confined twofold-degenerate electron, hh, and lh states of a single quantum well can split into a pair of symmetric and antisymmetric states.[15,20–23] The magnitude of splitting for each carrier type is determined by its effective mass and the accompanying band offset, as well as by well and barrier thicknesses. Due to its dependence on the effective mass, the amount of splitting is an individual parameter for each carrier type, and at a particular well and barrier width a situation can be created where only the carrier type with the smallest effective mass (e.g., electrons) exhibits coupling-induced splitting into symmetric and antisymmetric states. With the effective mass and the sample parameters known, the splitting directly yields the corresponding band offset. If, subsequently, at a constant well thickness the barrier width is reduced, the coupling of states with larger effective masses (e.g., hh's) is activated, and the corresponding band offset can be determined. Consequently, our method is explicitly sensitive to the band-offset ratio.

In this work the InAs layer and GaAs barrier thickness were accurately determined by high-resolution x-ray diffraction in a set of samples where at a constant InAs layer thickness of 1.1 ML the GaAs barrier width was varied from 4 to 32 ML. Subsequently, for all samples the splitting between symmetric and antisymmetric states was measured using PLE. All transitions observed in PLE were identified with respect to their hh and lh character by cleaved-side PLE. According to our model calculations, in a sample with a 32-ML barrier the splitting of the hh state is negligible due to its more than five times larger effective mass in comparison with the confined electron state. Consequently, the observed splitting of the hh exciton transition originates entirely from a splitting of the confined electron states, from which the conduction-band offset is directly being deduced. Once the conduction-band offset is known, the lh valence-band offset is derived from the coupling-induced splitting of the lh exciton transition simultaneously emerging in the 32-ML barrier sample, since the observed splitting is simply given by the sum of the splitting of the confined electron and confined lh states. Finally, with the known conduction-band offset, the hh band offset is determined from the splitting of the hh exciton transition and the accompanying strong redshift of the symmetric hh exciton transition in the 16-, 8-, and 4-ML barrier samples. In these samples the confined hh state also splits off into symmetric and antisymmetric states, and starts to contribute considerably to the observed redshift and splitting.

In the above-described method, uncertainties due to the excitonic character of the observed transitions are inherently eliminated. The strong dependence of the exciton binding energies on the InAs layer thickness is excluded, since in all samples the InAs layer was fixed to a thickness of 1.1 ML. Moreover, the band offsets are calculated from the observed splitting, i.e., from the energy difference of the observed transitions rather than from their absolute spectral position, so that the exciton binding energies cancel out.

When describing the electronic structure of single or coupled ultrathin InAs layers within the concept of band offsets, it is questionable whether the square-well model is the physically correct approach. The dominant criterion for the validity of the square-well model is that the envelope function is slowly varying on the scale of the lattice period.[24,25] As a consequence, part of the envelope function is still located inside the well, so that different effective masses in the direction of quantization have to be attributed to well and barrier. Finally, when increasing the well width, the square-well model will provide more than a single bound state. However, these assumptions strongly contradict the situation in ultrathin InAs layers. Moreover, in the band-offset determination reported previously, the assumptions had to be violated in order to achieve reasonable quantitative results by artificially attributing the GaAs effective masses of the barrier to the InAs well. Due to the confinement potential of a single InAs monolayer, the derivative of the envelope function will even change its sign within one lattice constant, i.e., as rapidly as the Bloch functions of the crystal, suggesting that the envelope wave function can only be constructed outside the InAs layer. The consequences of applying this conclusion are that the confined conduction- and valence-band states possess the effective masses of the GaAs barrier, and that increasing the InAs layer thickness will lead to a single bound state only.

In this work we introduce an alternative model for a description of the electronic structure of single and coupled ultrathin InAs layers, which still applies the concept of band offsets. By modeling the confinement potential of the InAs layers with Dirac's δ function, the main properties of the electronic structure are naturally considered: the use of a δ potential implies that the envelope function can only be constructed outside the InAs layer. Consequently, the effective masses of the bound electron, hh, and lh states are inherently fixed to the GaAs barrier values, and, finally, for each carrier type the δ potential provides only a single bound state regardless the thickness of the InAs layer. The imponderability that the δ potential is defined with a finite strength, without a clear physical meaning in the first place, can be overcome by a comparison of the eigenvalues of the δ potential with the eigenvalues of a square well providing the same strength in the limit case of a finite band offset and a well thickness approaching zero. A straightforward calculation shows that the strength of the δ potential equals the product of the InAs layer thickness and the actual band offset. As a result, the δ potential qualitatively and quantitatively provides the same physical correctness and precision as, e.g., the description by isoelectronic impurity layers.[26–28]

II. THEORETICAL MODEL

A. Description of the electronic structure by a δ-function potential

In order to extract the band offsets from the PL and PLE measurements, a model for the description of the electronic

structure in single and coupled ultrathin InAs layers in a GaAs matrix is required. The insertion of an InAs monolayer into a GaAs matrix corresponds to the isoelectronic substitution of Ga atoms by In atoms. In and Ga have the same chemical properties, but they differ in their atomic level position. Because no additional charge is introduced by the InAs plane, it induces a confining potential, which is localized on the length scale of the lattice constant, and which leads to the formation of confined electron, hh, and lh states in the GaAs band gap. Recently, Wilke and Hennig[29] described this situation of isoelectronic δ doping within the tight-binding scheme by using the Koster-Slater approach. One of the main conclusions of their work was that, as a consequence of the one-dimensional character of the GaAs conduction band near the Γ point, the electronic structure of ultrathin InAs layers in GaAs can still be treated in an effective mass approach. Moreover, they found that even for submonolayer coverages at least one In-related defect level with a hh character exists, but also that this number is not exceeded for coverages of more than 3 ML.

In this paper we present an alternative model for a description of the electronic structure, which, by applying the concept of band offsets, leads to the same qualitative and quantitative results as the model of isoelectronic impurities. We describe the confinement potential in the conduction and valence band by a δ function which can be written as $V(z) = -S_0\delta(z)$, where S_0 denotes the strength of the confining potential in the conduction and valence bands, and $\delta(z)$ is the Dirac function. The physical meaning of the strength parameter S_0 will be explained below. The most important inherent property of the δ potential is that no envelope function is constructed ''inside the well,'' and it is actually this property which gives the δ potential a preference among particle-in-a-box models when the potential width approaches the periodicity of the crystal Bloch wave functions. The crucial criterion for the validity of a particle-in-a-box model is that the envelope function varies slowly on the scale of the lattice period. However, in the case of ultrathin InAs layers, where the InAs layer modifies the atomic potential of the GaAs matrix on the length scale of the lattice constant, the derivative of the particle-in-a-box envelope function had to change its sign within one lattice period, which apparently contradicts the assumption. As a consequence of the fact that the wave functions extend entirely in the surrounding matrix, the δ potential implies that the effective masses of the confined states are given by the effective masses of the GaAs barrier in the direction of quantization. A further intrinsic property of the δ potential is that it provides only a single bound state regardless of the magnitude of S_0, which is consistent with the work of Ref. 29.

The calculations of the effective confinement energies and envelope functions of the bound valence-band states for a single ultrathin InAs layer have been carried out with the two-band Luttinger-Hamiltonian[30] in the spherical approximation ($\gamma_2=\gamma_3$),

$$\hat{H} = -\frac{\hbar^2}{2m_0}(\gamma_1+\tfrac{5}{2}\gamma_2)k^2 + 2\gamma_2(\hat{J}\cdot\hat{k})^2 - S_{\pm3/2,\pm1/2}\delta(z), \tag{1}$$

where we have chosen the z direction along the growth direction as the axis of quantization. Due to the δ-potential approach, the Luttinger parameters γ_1 and γ_2 are fixed to values of the GaAs barrier ($\gamma_1=6.85$, $\gamma_2=2.10$; see, e.g., Ref. 3). Furthermore, the use of the Luttinger Hamiltonian not only yields the correct effective masses of the bound states in the direction of quantization, which is determined by the confinement potential of the InAs layer, but also allows one to calculate the in-plane energy dispersion. In order to incorporate the compressive strain of the InAs layer in our model, we have chosen the strength parameter of the δ potential to be different for the hh subband ($S_{\pm3/2}$) and the lh subband ($S_{\pm1/2}$). Thus, implicitly, $S_{\pm3/2}$ and $S_{\pm1/2}$ both consider the same amount of hydrostatic strain as well as the strain-induced splitting of the hh and lh subbands due to the uniaxial strain component which is given by their difference. From Eq. (1) the effective confinement energies of the bound hh and lh states are straightforwardly derived as[31]

$$E_{\pm3/2,\pm1/2} = -\frac{m_0}{2\hbar^2(\gamma_1\mp2\gamma_2)}S^2_{\pm3/2,\pm1/2}. \tag{2}$$

The effective masses of the confined hh and lh states in the direction of quantization are identified as $m^*_{hh}=m_0/(\gamma_1-2\gamma_2)=0.3774m_0$ and $m^*_{lh}=m_0/(\gamma_1+2\gamma_2)=0.0905m_0$, respectively, which are exactly the values of the GaAs barrier that the δ-potential model predicts. For the conduction band, the calculation of the bound electron state yields the same expression as in Eq. (2), where one only has to replace $S_{hh,lh}$ with the strength of the conduction-band confinement potential S_e and the effective mass with the electron effective mass for GaAs: $m^*_e=0.0665m_0$. As a result, throughout the rest of this paper we proceed with the electron, hh, and lh effective masses as known, nonadjustable, parameters.

Before we present a description of the electronic structure of two coupled ultrathin InAs layers separated by a GaAs barrier, we first need to identify the physical meaning of the strength parameter S_0 of the δ potential. A relation between S_0 and the band offsets and the InAs layer thickness, respectively, can be found from a comparison between the eigenvalues of the δ potential and the eigenvalues of a square well providing the same strength in the limit of a finite potential depth and a well width approaching zero. For a square well, the potential depth V_0 can unambiguously be identified with the band offset ΔE, and the well width is identical to the thickness of the quantum-well layer, in the following denoted as a. Straightforwardly performing the limit case $a\to0$ yields the effective confinement energy for the bound state of such a shallow well as

$$E = -\frac{m^*}{2\hbar^2}a^2V_0^2 = -\frac{m^*}{2\hbar^2}a^2\Delta E^2. \tag{3}$$

From the comparison of Eq. (3) with the eigenvalues of the δ potential, it follows that the strength of the δ potential can be expressed by $S_0=aV_0=a\Delta E$. Thus, within the concept of band offsets, the effective confinement energies of the bound electron, hh, and lh states in ultrathin InAs layers can correctly be described by a δ potential, and they increase quadratically with the product of the corresponding band offset and the InAs layer thickness.

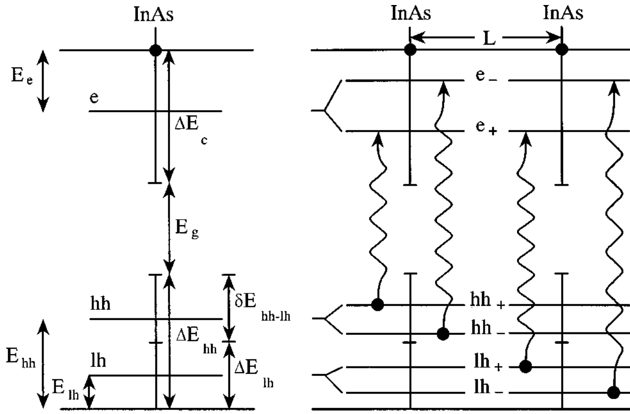

FIG. 1. Schematic real-space band alignment of a single ultrathin InAs layer of thickness a embedded in a GaAs matrix (left part), and two coupled InAs layers separated by a GaAs barrier (right part) of thickness L. The confined electron, hh, and lh states of the InAs layer are labelled as e, hh, and lh, and their effective confinement energies are denoted as E_e, E_{hh}, and E_{lh}. The strength of the confining potential, which is described by a δ potential, is determined by the conduction-band offset ΔE_c and the hh and lh band offsets ΔE_{hh} and ΔE_{lh}. The uniaxial strain component leads to a splitting $\delta E_{\text{hh-lh}}$ between the hh and lh valence subbands, which is considered by assuming different band offsets for the hh's and lh's. In the presence of coupling, each confined state splits off into a symmetric state (labeled as $+$) and an antisymmetric state (labeled as $-$). The parity-allowed transitions observed in PLE are indicated by the arrows.

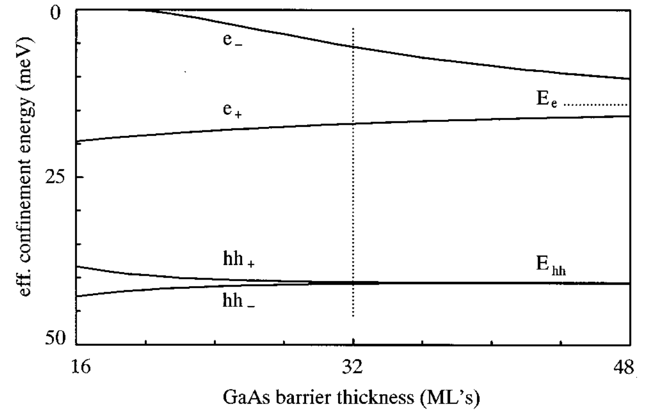

FIG. 2. Calculated electron and hh effective confinement energies for two coupled 1.1-ML-thick InAs layers as a function of GaAs barrier width using $\Delta E_c = 585$ meV, $m_e^* = 0.0665 \times m_0$, $\Delta E_{\mathrm{hh}} = 385$ meV, $m_{\mathrm{hh}}^* = 0.3774 \times m_0$. Thicknesses are given in units of the unstrained lattice constants of InAs (1 ML=3.0292 Å) and GaAs (1 ML=2.8266 Å). At $L = 32$ ML the splitting of the hh states is negligible, whereas the splitting of the electron states amounts to 13 meV. At approximately 20 ML the critical barrier thickness for the electrons is reached, where the e_- state becomes unbound.

B. Successive band-offset determination by means of two coupled InAs layers

For the samples containing two identical InAs layers separated by a GaAs barrier of thickness L, the effective-mass Hamiltonian in growth direction reads

$$\hat{H} = -\frac{\hbar^2}{2m^*}\frac{\partial^2}{\partial z^2} - aV_0\delta(z - L/2) - aV_0\delta(z + L/2). \quad (4)$$

In the limit case of infinite L the potential of the coupled InAs layers provides only a single bound state, whose effective confinement energy is the same as for the single InAs layer but which is twofold degenerate. As displayed in Fig. 1, when L becomes finite its degeneracy is lifted off, and it splits into symmetric antisymmetric states. The symmetric state corresponds to the ground state of the confining potential and it has an even symmetry, whereas the antisymmetric state corresponds to the first excited state with odd symmetry. By substituting $\kappa_\pm = \sqrt{-2m^* E_\pm/\hbar^2}$, where $\kappa_\pm$ has the meaning of the barrier penetration depth of the wave functions of the coupled-well problem, the energy eigenvalues E_+ and E_- of the symmetric and antisymmetric states are given by the two solutions of the characteristic equation

$$\frac{2m^* aV_0}{\hbar^2} = \frac{2\kappa_\pm}{1 \pm \exp(-\kappa_\pm L)}. \quad (5)$$

In the limit of an infinite barrier width, the eigenvalues of the symmetric and antisymmetric states become equal, and approach the value of a single δ potential. For the opposite limit case of a zero thickness barrier, the confinement energy of the symmetric state is equal to $E_+ = -2m^* a^2 V_0^2/\hbar^2$, which is identical to the effective confinement energy for a single InAs layer of double thickness. Therefore, when decreasing the barrier width, the symmetric state always remains bound, and its effective confinement energy increases. In contrast to that, the effective confinement energy of the antisymmetric state diminishes with decreasing barrier width, and at a critical barrier width of $L_c = \hbar^2/m^* aV_0$ the antisymmetric states becomes unbound.

In order to illustrate the evolution of the symmetric and antisymmetric states, in Fig. 2 we plot the effective confinement energy of the electron and heavy-hole states as a function of barrier width. Predominantly due to the difference in their effective masses by more than a factor of 5, for the displayed barrier widths both carrier types represent a different coupling regime. Calculating from Eqs. (2) and (3), the barrier penetration width of a single δ potential $\kappa = m^* aV_0/\hbar^2$ yields a value of $\kappa \approx 70$ Å for electrons corresponding to a 25-ML GaAs barrier, whereas the barrier penetration width of the hh's amounts to less than 20 Å (7-ML GaAs barrier). Thus in Fig. 2 the electrons represent the regime of moderate coupling ($\kappa \approx L$), and the hh's the situation for weak coupling ($\kappa \ll L$). In the latter case it is characteristic that the splitting between the symmetric and antisymmetric states is very small, and symmetrically distributed around the effective confinement energy of a single δ potential. For the electrons, however, the situation is different. The coupling-induced shift of the symmetric and antisymmetric states is no longer symmetric with respect to the bound state of a single δ potential. As can be seen from Fig. 2, the effective confinement energy of the antisymmetric state is already considerably altered, whereas that of the symmetric state has hardly changed. For later use it is also important to note that at a barrier thickness of 32 ML the hh's do not exhibit any splitting at all, whereas the splitting between the symmetric and antisymmetric electron states already amounts to 13 meV.

In PL or PLE one only observes optical transitions between states of equal parity. Thus, in the case of two coupled ultrathin InAs layers only the e_+-hh_+, e_--hh_-, e_+-lh_+, and e_--lh_- transitions will emerge (see Fig. 1). Considering that the observed transitions are excitonic ones, their transition energies are given by

$$E_{e_\pm\text{-hh}_\pm}=E_g^{\mathrm{GaAs}}+E_{e_\pm}+E_{\mathrm{hh}_\pm}-E_{\mathrm{hh}}^x,$$

$$E_{e_\pm\text{-lh}_\pm}=E_g^{\mathrm{GaAs}}+E_{e_\pm}+E_{\mathrm{lh}_\pm}-E_{\mathrm{lh}}^x, \qquad (6)$$

where E_{hh}^x and E_{lh}^x denote the hh- and lh-exciton binding energies, and $E_{\mathrm{hh}_\pm}$, $E_{\mathrm{lh}_\pm}$, and $E_{e_\pm}$ are the effective hh, lh, and electron confinement energies obtained from Eq. (5). From Eq. (6) it is evident that the observed splitting between the two hh- and lh-related transitions depends entirely on the band offsets ΔE_c, ΔE_{hh}, and ΔE_{lh}, once the effective masses and the thickness of the InAs layers and GaAs barrier are known. In turn, this provides a possibility to determine the values of the band offsets from the experimentally observed splitting. However, as can also be seen from Eq. (6), the observed splitting between the symmetric and antisymmetric transitions depends on both the splitting in the conduction band and the splitting in the hh and lh valence bands, respectively. In order to separate these contributions and thus to have direct access to the band-offset ratio, we developed a successive evaluation scheme for the band-offset determination which exploits the fact that the electron and hh effective masses differ by more than a factor of 5. As discussed above, a barrier thickness of 32 ML corresponds to approximately the barrier penetration width of the electrons, whereas it is still more than four times larger than the barrier penetration width of the hh's. As a consequence, at a 32-ML barrier width the hh_+-hh_- splitting is negligible as compared to the e_+-e_- splitting. Thus in this situation the splitting between the $e_+-\mathrm{hh}_+$ and e_--hh_- transitions observed in PLE is entirely due to the splitting in the conduction band, allowing for a direct determination of the conduction-band offset ΔE_c.

Once ΔE_c is known, the lh valence-band offset can be derived at the same barrier width from the splitting between the e_+-lh_+ and e_--lh_- transition, which is the sum of the splitting of the lh states and the just-determined splitting in the conduction band. Finally, the hh band offset can be determined from a sample where the barrier thickness becomes comparable to the hh barrier penetration width. Knowing the conduction-band offset and thus [from Eq. (5)] the splitting in the conduction band at any barrier width, the additional redshift of the e_+-hh_+ transition or the enhanced splitting between the e_+-hh_+ and e_--hh_- transitions directly yield ΔE_{hh}.

Finally we want to remark that our method of band-offset determination is insensitive to excitonic effects. In previous papers, the band offsets were extracted from the dependence of the *absolute spectral position* of the hh- and lh-exciton transitions on the thickness of a single InAs layer. Since, e.g., the hh-exciton binding energy was found to increase[6] from 4 meV at zero InAs layer thickness to 12 meV at an InAs layer thickness of 1.6 ML, this method requires a sound knowledge of the dependence of the hh- and lh-exciton binding energies on the InAs layer thickness. In contrast to that, in a set of samples where the InAs layer thickness was kept constant, we deduce the band offsets from the splitting of the excitonic $e_\pm$-$\mathrm{hh}_\pm$ and $e_\pm$-$\mathrm{lh}_\pm$ transitions, i.e., from their *difference in spectral position*. As is evident from Eq. (6), in this approach the exciton binding energies cancel out. The only remaining uncertainty is a possible variation of the exciton binding energy as a function of barrier thickness. However, from calculations of the exciton binding energies as a function of barrier width for the regime of weak and moderate couplings, we find that the changes in the exciton binding energies are smaller than 3 meV, which is small enough not to add significant uncertainty to the values of the band offsets we determine.

III. SAMPLE GROWTH AND STRUCTURAL CHARACTERIZATION

The samples under investigation contain two ultrathin InAs layers separated by a GaAs barrier with nominal thicknesses of 4, 8, 16, and 32 ML, respectively. Within this set of samples an additional reference sample was grown which comprises a single InAs layer only. The samples were synthesized by conventional molecular-beam epitaxy on an exactly oriented CrO-doped semi-insulating (001) GaAs substrate. After oxide desorption, a 0.4-μm GaAs buffer layer was grown at a substrate temperature of 630 °C. Then the substrate temperature was lowered to 600 °C, and the As-cracker temperature was set to 400 °C to grow with As_4. At this substrate temperature a 400-Å GaAs layer was grown followed by an additional 350-Å-thick GaAs layer within which the substrate temperature was lowered to 450 °C. This temperature ramp was found to be optimum to achieve a high optical quality GaAs matrix. Subsequently, the two ultrathin InAs layers and the GaAs barrier were deposited at 450 °C. Before and after the deposition of each InAs layer, a 1-s growth interrupt was introduced to allow surface reconstruction and to suppress the formation of InAs clusters.[32–34] The intended thickness of each InAs layer was 1 ML. After the growth of the second InAs layer, 5 ML of GaAs were deposited. Subsequently, while growing a 565-Å GaAs cladding layer, the substrate temperature was increased to 630 °C. Finally, a 300-Å $\mathrm{Al}_{0.33}\mathrm{Ga}_{0.67}\mathrm{As}$ window was grown to suppress surface electric fields, and the structures were capped by a 170-Å GaAs layer. To avoid any possible source of external strain, the substrates were mounted free of ln on the substrate holder. For the x-ray-diffraction and optical measurements, the samples were held by paper frames on the sample holder.

As mentioned in Sec. II [see Eq. (5)], the band offsets can only be derived if the InAs layer and GaAs barrier thickness are precisely known. Consequently, on each sample we performed high-resolution double-crystal x-ray-diffraction measurements, which allowed us to determine the thickness of ultrathin InAs layers with an accuracy of better than 0.1 ML.[35] The x-ray experiments were performed in the symmetric (400) geometry utilizing the Cu $K\alpha_1$ line. The InAs layer and the GaAs barrier thickness were found from a comparison between the measured rocking curves and their simulations based on the dynamical theory.

In Fig. 3 we plot the measured rocking curve (bottom) and simulations (top) for a single InAs layer (a), for samples

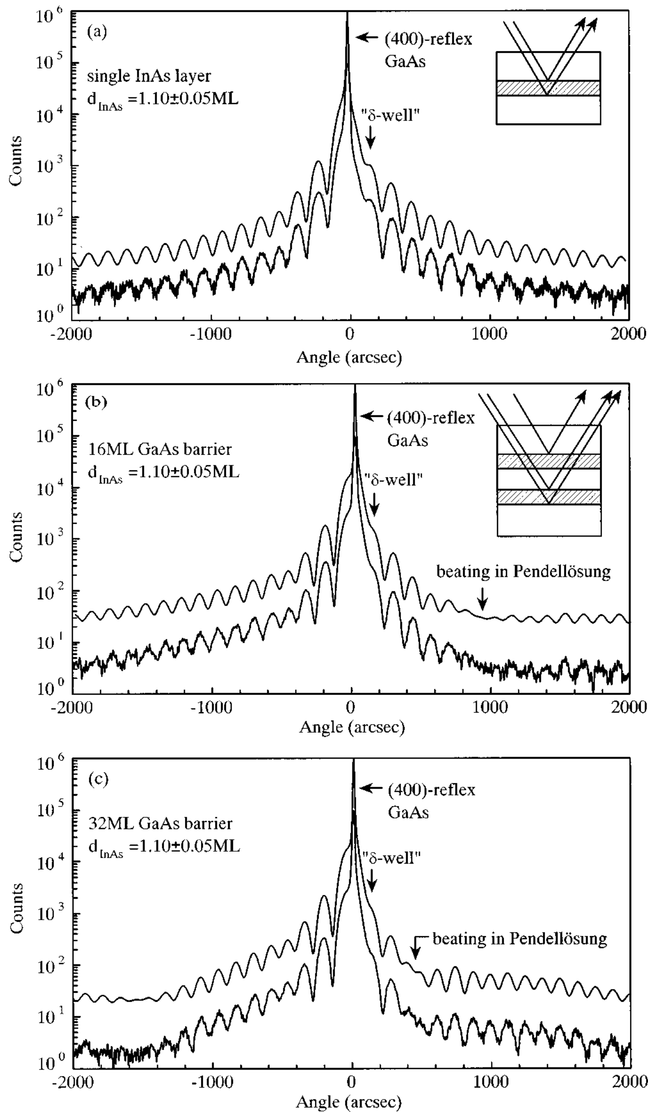

FIG. 3. Measured (lower curves) and simulated (upper curve) rocking curves of the reference sample (a) containing a single InAs layer and two samples with 16-ML (b) and 32-ML (c) GaAs barriers between the two InAs layers. The feature in the simulated rocking curves which is most sensitive to the composition of the InAs layer is denoted as the ''δ well.'' In the rocking curves of the 16- and 32-ML barrier samples, a destructive interference of the Pendellösung occurs, whose angular position is determined by the GaAs barrier thickness. For the whole set of samples the InAs layer thickness was consistently found to be 1.10 ± 0.05 ML. The thickness of the GaAs barriers are given in the figure.

with a 16-ML (b) and 32-ML (c) GaAs barrier, respectively. As indicated in the inset of Fig. 3(a), in the case of a single InAs layer the incident x-ray field is diffracted simultaneously from the underlying GaAs layer and from the cap layer comprising the upper GaAs layer and the $Al_xGa_{1-x}As$ window at identical Bragg angles. The interference between both contributions is observed by the Pendellösung oscillations, whose modulation amplitude and angular position are determined by the thickness of the InAs layer and the incorporated amount of strain. The features in the rocking curve of the single InAs layer [Fig. 3(a)], which is most sensitive to the InAs layer thickness, are the position and shape of the Pendellösung fringe close to the substrate peak denoted as the δ well. From the simulations we find an average thickness of the InAs layer of 1.10 ± 0.05 ML. The best fit was obtained with a zero in-plane strain and 6.8% strain in the (100) direction. This provides evidence that the lattice mismatch is fully accommodated by an elastic distortion of the InAs unit cell, i.e., the InAs layer is grown pseudomorphically.[36]

The significant feature in the rocking curves of the coupled InAs layers [Figs. 3(b) and 3(c)] is the appearance of a destructive interference of the Pendellösung oscillations. As depicted in the inset of Fig. 3(b), the x-ray field from the underlying GaAs layer can interfere with the x-ray field from the upper GaAs layer and the $Al_xGa_{1-x}As$ window as well as with the x-ray field, which is diffracted from the layer stack comprising the upper GaAs layer and the $Al_xGa_{1-x}As$ window plus the two InAs layers and the GaAs barrier. Both interferences lead to Pendellösung oscillations with a slightly different periodicity. The superposition of these Pendellösung oscillations gives rise to the observed beating. The simulations show that a ±1-ML change of the barrier thickness shifts the angular position of the beating in the Pendellösung considerably (by approximately ±50 arcsec), whereas the feature close to the substrate peak (denoted as the δ well) remains unchanged. In contrast to that, a small change in the InAs layer thickness, i.e., in the amount of totally deposited InAs, hardly changes the position of the beating in the Pendellösung, but considerably alters the feature near the substrate peak. Consequently, the simulations of the measured rocking curves for the coupled-well samples allow us to determine the GaAs barrier InAs layer thickness almost independently. For the whole set of samples we consistently find an average InAs layer thickness of 1.10 ± 0.05 ML. The barrier thickness were found to be 4, 8, 16, and 32 ML, respectively, with an uncertainty of ±0.5 ML.

With respect to the above description of the electronic structure of the InAs layer by a δ potential, and the question of over how many atomic layers the deposited InAs is distributed, our simulations reveal the following results. The InAs layer thickness obtained above assumes a pure InAs layer. However, a similar quality of the simulation for the single InAs layer sample can be obtained when the InAs layer is decomposed into 1-ML InAs and 1-ML $In_{0.05}Ga_{0.95}As$ on either side. This result is not too surprising, since the angular position of the Pendellösung oscillations and the shape of the δ-well feature depend on the product of the total amount of deposited InAs and the totally incorporated amount of strain. Thus, as long as the total InAs content in the simulations of the single InAs layer sample is kept constant within the $\pm5\%$ variation of the found layer thickness, the rocking curves do not provide accurate information about the distribution of the InAs over one or more atomic layers. Nevertheless, an estimate of how much InAs is confined in a single atomic layer can be obtained from the rocking curves of the samples with 16- and 8-ML barrier thicknesses. In simulations of these samples, we decomposed the InAs layers into two or three adjacent $In_xGa_{1-x}As$ monolayers with different In contents by keeping the total amount of InAs constant. When the In contents in the $In_xGa_{1-x}As$ layers was brought toward an equidistribution, a shift of the beating in the Pendellösung oscillations by more than 200 arcsec toward the substrate reflection is observed. In order to

match the simulations with the measured rocking curves, this shift could only be compensated for by reducing the barrier thickness by 4 ML. However, as will be discussed in Sec. IV, especially for small barriers (8 and 16 ML), such a strong reduction of the barrier thickness would lead to a redshift of the photoluminescence by more than 20 meV, which would be in contradiction to our optical experiments. In turn, if we allow the barrier thickness to be determined as 1 ML too wide (corresponding to less than a 5-meV redshift of the PL), we find, in agreement with the work of Woicik *et al.*,[36] that still more than 80% of the deposited InAs is confined in one atomic plane. Additional information, i.e., whether the residual InAs is symmetrically or asymmetrically distributed around the layer containing more than 80% of the deposited InAs, could not be found. Finally, it should be mentioned that the rocking curves do not show any indication of strain relaxation, although the total amount of InAs in our structures (2.2 ± 0.1 ML) is very close to the critical layer thickness of a single InAs layer.

IV. RESULTS

PL and PLE measurements were carried out in backscattering geometry using a tuneable Ti:sapphire laser with a linewidth of less than 0.25 meV and a (2×0.85)-m double monochromator with a spectral resolution of better than 0.2 meV. The observed transitions were identified with respect to their hh and lh characters[5,37] by cleaved side PLE measurements, where the freshly cleaved side of the samples was excited with either *s*- or *p*-polarized light, and the PL emission (I_s,I_p) was detected in the direction perpendicular to the sample surface. By defining the degree of polarization (DOP) as $(I_s-I_p)/(I_s+I_p)$, positive values indicate that the valence-band states involved in the transitions are hh-like, whereas negative values indicate a lh character.

The 4.2-K PL spectra of the single and coupled InAs layer samples are shown in Fig. 4. The observed PL originates from the e_+-hh_+-exciton transition as the lowest-lying transition of the InAs layers. The PL intensity and the peak intensity ratio between the PL from the InAs layers and the GaAs exciton of approximately 100 is almost equal for all samples, indicating that the exciton binding energy is hardly altered by the coupling of the InAs layers. The full width at half maximum (FWHM) of the PL emission amounts to 8.5 meV in the single InAs layer and varies nonsystematically between 5.9 and 8.4 meV for the coupled InAs layers. Previous studies of the FWHM in InAs monolayers[33] have shown that growth interrupts <10 s result in a uniform distribution of the InAs and not in the formation of InAs islands of different sizes. This is consistent with recent measurements of the dephasing times in ultrathin InAs layers, which show that lateral potential fluctuations experienced by the excitons take place on a length scale larger than the exciton Bohr radius.[39] In addition, consistent with our x-ray analysis, the PL spectra do not show indications of strain relaxation, showing that a 4-ML GaAs barrier is thick enough to keep the growth of the second InAs layer pseudomorphic.

When the barrier thickness is reduced from 32 to 4 ML, we observe a redshift of the PL line of 54 meV. Since the change in exciton binding energy of the symmetric e_+-hh_+ transition is smaller than 3 meV over the entire range of barrier widths, this redshift originates predominantly from the increase in the effective confinement energies of the e_+ and hh_+ states. The observed redshift is in excellent agreement with our model calculations (indicated by the arrows in Fig. 4) as well as with the tight-binding calculations from Wilke and Hennig,[29] who predicted a redshift of 50 meV.

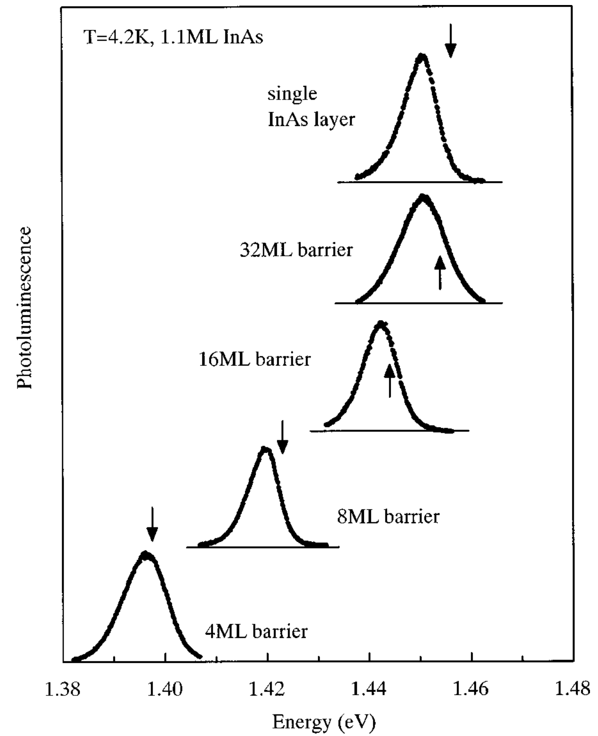

FIG. 4. 4.2-K photoluminescence spectra of the single InAs layer sample and the samples containing two InAs layers separated by a GaAs barrier of 4, 8, 16, and 32 ML, respectively. For clearer presentation each PL spectrum was given an arbitrary offset. The spectral position of hh-exciton PL is identically for the single InAs layer and the 32-ML barrier sample. When the barrier thickness is reduced from 32 to 4 ML, the hh-exciton PL is redshifted by 54 meV. Note that neither a systematic line broadening nor a systematic change in line intensity is observed when the barrier width is decreased. The arrows indicate the calculated transition energies using the δ-potential model, without a correction for the hh-exciton binding energy.

With respect to the separation of the conduction- and valence-band offsets, it is important to note that the energy separation between the PL line of the single InAs layer and 32-ML barrier sample is less than 1 meV. However, this small energy separation in PL does not necessarily imply the absence of coupling. As Fig. 2 reveals, at a 32-ML barrier thickness the effective confinement energy of the hh state is not altered at all, and the effective confinement energy of the e_+ state is hardly increased, whereas the effective confinement energy of the e_- state is decreased by almost 10 meV. As the PLE measurements discussed in Sec. V will show, a 32-ML GaAs barrier leads to considerable coupling for the bound-electron states which is almost completely accumulated in a blueshift of the antisymmetric e_- state.

The PLE and cleaved side PLE measurements of the samples are shown in Figs. 5 and 6, respectively. In the PLE spectrum of the single InAs layer two peaks are visible, which are the hh-exciton transition at 1.4565 eV and the

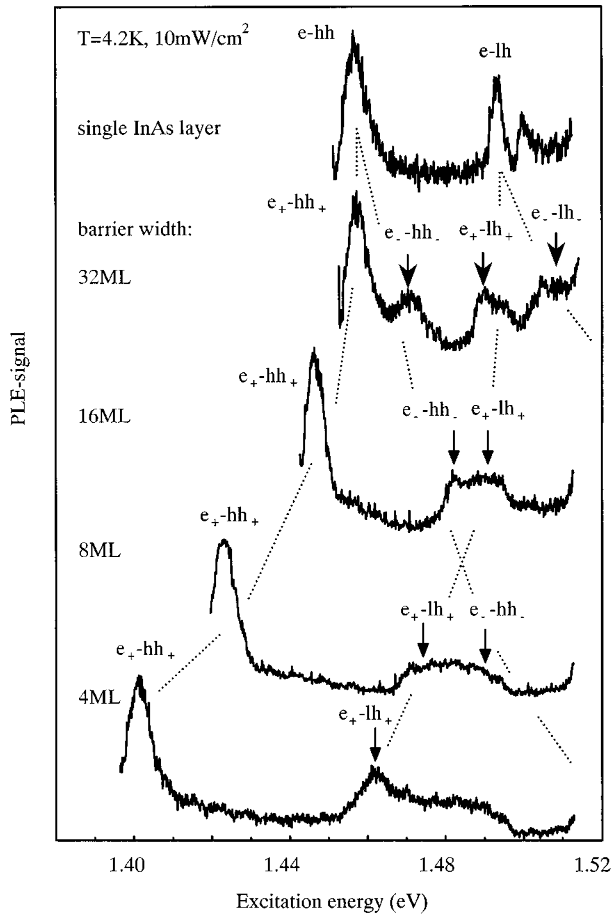

FIG. 5. PLE spectra of the samples measured at 4.2 K in backscattering geometry. The transitions were identified with respect to their hh and lh character by cleaved side PLE measurements. In the PLE spectrum of the single InAs layer, the hh- and lh-exciton transitions (denoted as e-hh and e-lh) are clearly visible. In the 32-ML barrier sample, four parity-allowed transitions emerge, demonstrating the coupling between the two InAs layers. Note that in the 32-ML sample the e_+-hh$_+$ transition emerges at almost the same spectral position as the e-hh transition in the single InAs layer.

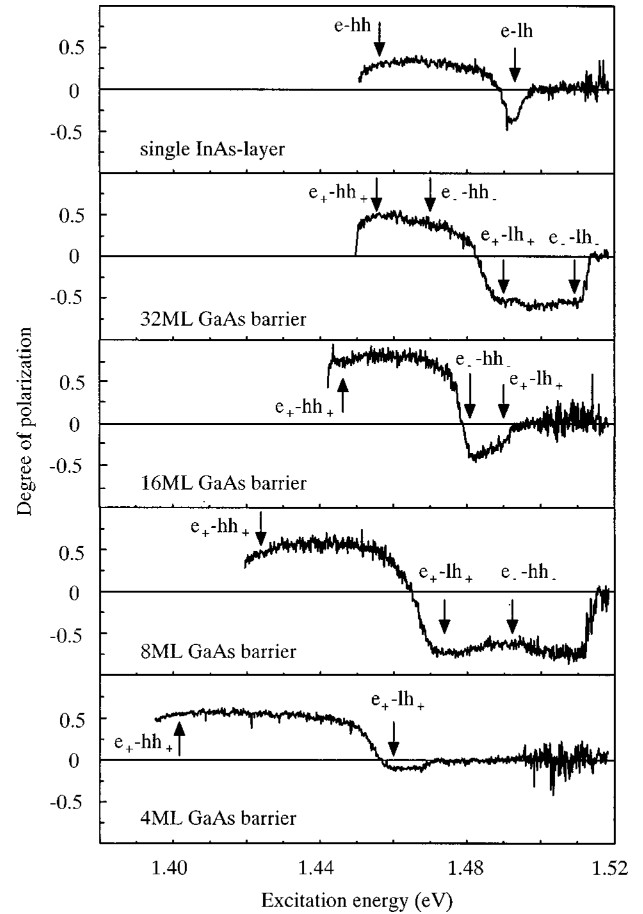

FIG. 6. Cleaved side PLE spectra of the samples measured at 4.2 K. A positive degree of polarization indicates a hh character of the valence-band states involved in the transitions observed in PLE (indicated by the arrows), whereas negative values show the lh character.

lh-exciton transition at 1.4930 eV. In particular the origin of the latter was carefully checked, since it is close to the carbon-related donor-to-acceptor transition in GaAs. As it can be seen from Fig. 6, our cleaved side PLE measurements show a strong p polarization at this energy, whereas Brandt *et al.*[5] found a hh character for the carbon-related transition. A steplike structure, with a peak on top between 1.4985 and 1.51 eV, results from the two-dimensional density of states of the e-lh band-to-band transition and the absorption by excited and unbound lh-exciton states. From this feature we deduce a lh-exciton binding energy of 5.5 meV. In contrast to this, we do not resolve a similar contribution to the absorption from the e-hh band-to-band transition. In our opinion this is due to the fact that the strength of the band-to-band absorption is determined by the in-plane effective masses ($m_\parallel^*$), which from Eq. (1) is found to be more than two times smaller for the hh's ($m_{\parallel \mathrm{hh}}^* \cong 0.155 m_0$) as compared to the lh's ($m_{\parallel \mathrm{lh}}^* \cong 0.362 m_0$). In addition, we determined the hh-exciton binding energy by temperature-dependent PL measurements, and found a value of 10 meV.

The coupling between the two InAs layers is clearly visible in the PLE spectrum of the 32-ML barrier sample, where we resolve four peaks. Considering that only transitions between states of equal parity are observed, they were identified by their polarization properties (see Fig. 6) as the e_+-hh$_+$, e_--hh$_-$, e_+-lh$_+$, and e_--lh$_-$ excitonic transitions. The observed splitting between the e_+-hh$_+$ and e_--hh$_-$ transition amounts to 13 and 19 meV between the e_+-lh$_+$ and e_--lh$_-$ transitions, respectively.

According to Sec. III, each of these splittings is the sum of the e_+-e_- splitting and the hh$_+$-hh$_-$ or lh$_+$-lh$_-$ splitting, respectively. The most important requirement for the separation of the contributions from the conduction and valence bands and the successive determination of the band offsets was a negligible splitting between the hh$_+$ and hh$_-$ states in the regime of weak coupling. This assumption is justified by the following observations in the PL and PLE spectra of the 32-ML barrier sample.

(i) In both the 32-ML barrier sample and single InAs layer sample, the energy difference between the e_+-hh$_+$- or e-hh-exciton transition is the same, in PL as well as in PLE. This means that the hh-exciton binding energies and the Stokes shift are both either not altered at all or that their changes are small and exactly compensate for each other. Thus, although the transitions are excitonic ones, the observed 13-meV splitting is only affected by the splitting of the confined e and hh

states, and contributions of the exciton binding energy of Stokes shift cancel out.

(ii) In both PL and PLE, the e_+-hh$_+$ transition of the 32-ML barrier sample emerges at the same spectral position as the e-hh transition of the single InAs layer sample. This observation is in agreement with our calculations shown in Fig. 2, which reveal that at a 32-ML barrier thickness the shift of the hh$_+$ level with respect to the hh level is virtually zero, and the shift of the e_+ level with respect to the uncoupled case is very small.

(iii) Figure 2 also shows that the coupling-induced shift of the antisymmetric e_- state is much larger than the shift of the symmetric e_+ state, and that most of the e_+-e_- splitting is accumulated in a shift of the e_- state since the confined electron states are in the regime of moderate coupling ($\kappa_e \approx L$). In contrast to this, since the effective mass of the hh's in the direction of quantization is five times higher than the one of the electrons, the hh states represent the regime of weak coupling ($\kappa_{\mathrm{hh}} \ll L$). Consequently, in the 32-ML barrier sample not only is the shift of the hh$_+$ state negligible, but so is the hh$_+$-hh$_-$ splitting.

From the above discussion we can conclude that the observed splitting between the e_+-hh$_+$ and e_--hh$_-$ transition originates entirely from the e_+-e_- splitting in the conduction band. Since the InAs layer thickness, the barrier thickness, and the electron effective mass are known, by applying Eq. (5) we obtain, from the 13-meV e_+-e_- splitting, a conduction-band offset of $\Delta E_c = 535 \pm 15$ meV. The uncertainty in the conduction-band offset results from the uncertainty in the InAs layer thickness (± 0.05 ML) and the GaAs barrier thickness (± 0.5 ML). Knowing the splitting of the confined electron states, the lh band offset can be extracted from the same PLE spectrum. Since the 19-meV splitting between the e_+-lh$_+$ and e_--lh$_-$ transitions is the sum of the e_+-e_- and lh$_+$-lh$_-$ splitting, the lh$_+$-lh$_-$ splitting alone amounts to 6 meV. By again applying Eq. (5) and using the lh effective mass, we find a lh valence band offset of $\Delta E_{\mathrm{lh}} = 225 \pm 25$ meV. The larger uncertainty in the lh valence-band offset is due to the somewhat broader $e_\pm$-lh$_\pm$ transitions. By performing similar calculations to those displayed in Fig. 2 for the lh$_+$ and lh$_-$ states, we find an increase of the effective lh$_+$ confinement energy by 3 meV as compared to the uncoupled case. By comparing this value with the 3.5-meV redshift of the e_+-lh$_+$ transition observed in the 32-ML barrier sample, the magnitude of ΔE_{lh} was verified. The fact that the lh$_+$-lh$_-$ splitting is equally distributed in the shift of the lh$_+$ and lh$_-$ states is a consequence of the much weaker lh confinement as compared to the hh's, in combination with the fact that the lh states are in regime of strong coupling ($\kappa_{\mathrm{hh}} \gg L$). With $\Delta E_{\mathrm{lh}} = 225$ meV and $m^*_{\mathrm{lh}} = 0.0905 m_0$, the lh localization length amounts to 124 Å (44 ML), which is already considerably larger than the barrier width. Thus in coupled ultrathin InAs layers the coupling of the lh's is stronger than for the electrons and hh's. It should be noted that the weak lh confinement is not only the result of the smaller lh effective mass as expressed in Eq. (2). In addition, the small lh band offset we find is a direct consequence of the shear strain component, which under compressive strain leads to a diminishing of the band offset for the lh's as compared to the hh band offset.

Finally, we determined the hh valence-band offset from the observed 10-, 33-, and 54-meV redshifts of the e_+-hh$_+$ transition in the 16-, 8-, and 4-ML barrier samples with respect to the uncoupled case. Since the barrier width in these samples reaches the value of the hh barrier penetration length, the redshift of the e_+-hh$_+$ transition is now due to the increase of the effective confinement energy of both, the hh$_+$ and e_+ states. With the conduction-band offset known, we obtain a hh valence-band offset of 385 ± 15 meV. With the values for the conduction and hh band offsets, we experimentally find a band-offset ratio of $Q_c = 0.58$.

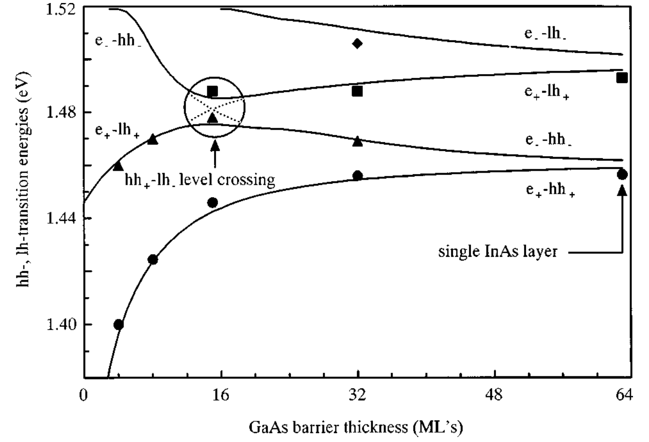

FIG. 7. Measured and calculated transition energies for the coupled InAs layer samples as a function of barrier width. The calculations were performed using $\Delta E_c = 585$ meV, $\Delta E_{\mathrm{hh}} = 385$ meV, and $\Delta E_{\mathrm{lh}} = 225$ meV. The symbols at 64 ML represent the transitions observed in the single InAs layer. At around 16 ML one observes a crossover between the e_+-lh$_+$ and e_--hh$_-$ transitions.

An overview of the transitions measured in the whole set of samples by PLE and the calculation of the transition energies as a function of barrier thickness, using our δ-potential model and the band offsets determined above, is displayed in Fig. 7. The agreement between experiment and theory supports the validity of our band offsets and the δ-potential approach. An interesting feature emerges at a barrier thickness of approximately 16 ML, which in Fig. 7 is denoted as "hh$_-$-lh$_+$ crossing." At this barrier thickness, in the PLE spectrum an 18-meV broadband centered at 1.488 eV is visible rather than two separate peaks. As a consequence we did not consider the splitting between the e_+-hh$_+$ and $e_- -$hh$_-$ transitions for the determination of ΔE_{hh}. In addition, the cleaved side PLE spectrum of this sample reveals p polarization for this band. The origin of this band can be explained as follows: when the barrier thickness is reduced, the effective confinement energy of the symmetric states is increased (redshift), whereas the effective confinement energy of the antisymmetric states decreases (blueshift) until the critical barrier thickness is reached, where they become unconfined. An indication that the latter has certainly happened to the lh$_-$ state is the fact that the PLE spectrum of the 16-ML barrier sample above 1.495 eV is completely structureless, and that the measured PL background is completely unpolarized. At a barrier thickness of approximately 16 ML, the effective confinement energy of the blueshifted lh$_+$ state and the redshifted hh$_-$ state become equal, so that both levels cross each other. At the crossover point the energy sepa-

ration between the e_--hh$_-$ and e_+-lh$_+$ transition is entirely determined by the splitting between the e_+ and e_- states, which according to Fig. 2 amounts to 19 meV. The DOP in the crossover region is given by the superposition of the polarization properties of the e_--hh$_-$ and e_+-lh$_+$ transitions, i.e., it depends on the ratio between σ and π components of each transition weighted by their oscillator strength. As it can be seen from the cleaved side PLE spectrum of the 32- or 8-ML barrier samples, the DOP for the hh transitions (see, e.g., the e_+-hh$_+$ transition) is reduced from its theoretical value of $+1$ at the expense of a weaker σ component, whereas the DOP of the lh transitions (see, e.g., the e_+-lh$_+$ transition) is increased with respect to its theoretical value of $-\frac{1}{3}$ in favor of the π component. Assuming equal oscillator strengths for the e_--hh$_-$ and e_+-lh$_+$ transitions, their superposition leads effectively to a negative DOP at the crossover point. That the crossing of the hh$_-$ and lh$_+$ levels indeed occurred becomes evident from a comparison of the PLE and cleaved side PLE spectra of the 32-ML barrier sample with the ones of the 8- or 4-ML samples. For the 32-ML sample the second-lowest-lying transition is the e_--hh$_-$ transition at 1.47 eV, identified by its strong s polarization. In contrast to that, in the 8- and 4-ML samples where the e_--hh$_-$ and e_+-lh$^+$ transitions are again spectrally well separated, the second-lowest-lying transition is predominantly p polarized, indicating that both transitions crossed each other and that the lh$_+$ level has become the first excited valence-band state of the two coupled InAs layers.

The remaining question, concerning at which barrier thickness the antisymmetric electron state becomes unconfined, cannot be answered conclusively. The calculation in Fig. 2 reveals that the critical barrier thickness for the electrons is reached at approximately 20 ML. However, these calculations do not include a repulsive interaction between the antisymmetric electron state and the GaAs conduction band, which would shift the critical barrier thickness for the electrons toward smaller barrier widths. The broadband at 1.488 eV in the PLE spectrum of the 16-ML sample seems to contain the e_+-lh$_+$ transition as well as the e_--hh$_-$ transition, both having equal oscillator strengths. This would indicate that the e_- state is at least still in strong resonance with the GaAs conduction band, but not completely unconfined.

V. DISCUSSION

In this section we compare our results for the band offsets with elasticity theory and the experimental results of other groups. With the band offsets obtained above we determine a band gap for the strained InAs layer of $E_g^{\mathrm{InAs}}=0.6\,\mathrm{eV}$ by applying

$$E_g^{\mathrm{InAs}}=E_g^{\mathrm{GaAs}}-\Delta E_c-\Delta E_{\mathrm{hh}}. \tag{7}$$

Since in our δ-potential approach this value is used in the sense of a bulk parameter, one has to compare it with the value derived from macroscopic elasticity theory,

$$E_g=E_g^0+\delta E_{\mathrm{hy}}+\delta E_{\mathrm{sh}}, \tag{8}$$

which recently was found to describe InAs/GaAs films even in the monolayer limit.[36] In Eq. (8), E_g^0 denotes the band gap of unstrained InAs, and δE_{hy} and δE_{sh} are the hydrostatic and shear strain energy components, respectively. In the case of a uniaxial strain component in the (100) direction, these are given by[13,14]

$$\delta E_{\mathrm{hy}}=2\alpha(1-C_{12}/C_{11})\varepsilon,$$

$$\delta E_{\mathrm{sh}}=-\beta(1+2C_{12}/C_{11})\varepsilon. \tag{9}$$

Assuming that the InAs layer is 6.8% compressively strained, and taking the values for the hydrostatic deformation potential α, the shear deformation potential β, and the stiffness constants C_{12} and C_{11} reported elsewhere,[3,13] one finds a band gap for the strained InAs layer of 0.573 eV. Our experimentally determined value for the band gap of 0.6 eV is thus in agreement with elasticity theory.

For the discussion of the lh confinement and the splitting between the hh and lh subbands due to the uniaxial strain, one has to keep in mind that in our δ-potential model the strain-induced splitting between the hh and lh subbands is taken into account by assuming different band offsets ΔE_{hh} and ΔE_{lh}. Thus any alteration of the band alignment due to the split-off band, which in ultrathin and highly strained layers becomes important, is considered implicitly. Furthermore, changes of the band structure due to strain fields in the surrounding GaAs matrix are neglected.

Alterations of the valence-band structure by the split-off band are known for highly strained quantum wells and bulk material as well as for unstrained quantum wells, which are only a few monolayers wide. In both cases the split-off band only affects the lh subband but not the hh subband. In ultrathin InAs layers both effects have to be considered.

(i) Due to the 6.8% compressive strain in the InAs layer, the shear strain energy component δE_{sh} is not small compared to the energy of the split-off band Δ_0. As a consequence, the approximation usually made, that the strain-induced energy separation between the hh and lh band offsets amounts to $2\delta E_{\mathrm{sh}}$ is no longer valid, but has to be replaced with the expression[14]

$$\delta E_{\mathrm{hh\text{-}lh}}=\tfrac{1}{2}(3\,\delta E_{\mathrm{sh}}-\Delta_0)+\tfrac{1}{2}\sqrt{\Delta_0^2+2\Delta_0\delta E_{\mathrm{sh}}+9\,\delta E_{\mathrm{sh}}^2}, \tag{10}$$

which yields a value for $\delta E_{\mathrm{hh\text{-}lh}}$ of 206 meV. From the band offsets determined above, we find an experimental value of $\delta E_{\mathrm{hh\text{-}lh}}=160\,\mathrm{meV}$. Although both values are in reasonable agreement, one can at least qualitatively explain why the experimental value is too small. With the lh band offset as derived above, the effective confinement energy of the confined lh's amounts to 3 meV. For such a weak confinement close to the GaAs valence band, one has to expect a repulsion between the confined lh level and the GaAs valence band due to their identical symmetry. Effectively this would appear as a slightly stronger confinement of the lh's. How-

ever, in our calculations this repulsive interaction is not considered explicitly, but only implicitly by a slight overestimate of the lh band offset.

(ii) The second influence of the split-off band on the band alignment in ultrathin InAs layers results entirely from the fact that the InAs layer is only 1 ML wide. Recently, Dujardin, Marréaud, and Laurenti[38] demonstrated that even in the case of lattice-matched ultrathin quantum wells the effective lh confinement energy is underestimated when the split-off band is not taken into account. Using a 6×6 Hamiltonian, they calculated that in a 1-ML-wide well, where the confinement energy becomes comparable with Δ_0, the effective confinement energy of the lh's will be determined as much as 10 meV too low when the interaction with the split-off band is neglected, whereas the effective hh confinement energy remains unchanged. Since in our calculations of the effective lh confinement energy the split-off band is not included, the lh band offset is overestimated to account for the increase of the effective lh confinement energy due to spin orbit coupling.

The main difference between our band offsets and the results of other groups is the magnitude of lh confinement. With the values for the lh band offset reported by Wang *et al.*[6] (89 meV) and in Refs. 3 and 6 (30–35 meV), one finds effective lh confinement energies of 0.4 and 0.1 meV, respectively. As a consequence, these small lh band offsets lead to the conclusion that, at 4 K, the lh state is practically delocalized and the corresponding exciton is unbound. However, our lh band offset of 225 meV provides an effective confinement energy ten times higher, which at low temperatures is sufficient to keep the lh state localized and thus gives rise to a bound lh exciton state. This result is in very good agreement with the observation of a bound lh exciton in the PLE spectrum of the single InAs layer (see Fig. 5). In addition, direct proof of the existence of a confined lh state and, subsequently, a bound lh exciton was recently obtained in a slightly thicker (1.2 ML) InAs layer, where the energy separation between the hh and lh excitons amounts to one GaAs LO phonon.[39] In that sample a sharp line originating from resonant luminescence and doubly resonant Raman scattering is observed in addition to regular hh-exciton PL, when the exciting laser beam is tuned on the lh exciton transition. This sharp line remains present up to temperatures of 18 K, which requires an effective lh confinement energy of larger than 1.5 meV.

In order to see whether our band offsets and our δ-potential model are suitable to describe the electronic structure of ultrathin InAs layers in a GaAs matrix over the whole range of the two-dimensional growth regime, we calculated the transition energies for hh and lh transitions with our band offsets as a function of the InAs layer thickness. This calculation is displayed in Fig. 8 together with the experimental results of other groups.[3,4,6,40] As can be seen from the figure, our calculation is in good agreement with the experiments. However, it should be noted that the agreement can be improved when the dependence of the hh- and lh-exciton binding energy on the InAs layer thickness is taken into account. This is displayed in Fig. 8 by the dotted lines. Here the InAs layer thickness dependence of the exciton binding energies was calculated using the zero-radius potential model.[6,19]

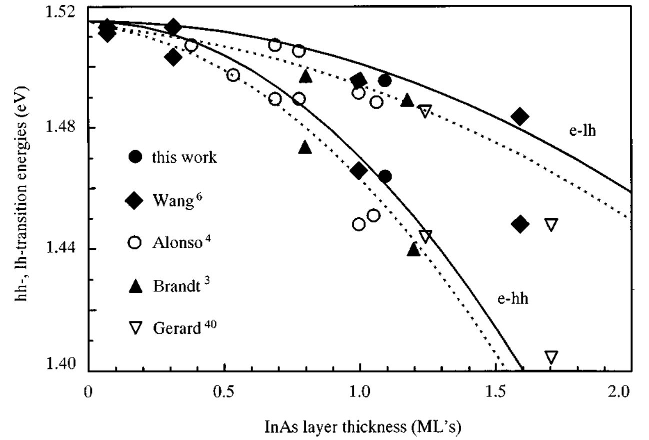

FIG. 8. Observed and calculated transition energies for a single InAs layer as a function of the InAs layer thickness. The calculations (solid lines) are based on the δ-potential model, with the band offsets determined in this paper. The experimental data were taken from literature. The dotted lines show the calculations including the dependence of the exciton binding energy on InAs layer thickness according to the zero-radius potential model.

Finally we would like to point out that, for the dependence of the transition energies on the InAs layer thickness, the same quality of agreement between experimental and calculated transition energies was achieved previously by other groups, but with very different sets of band offsets, since they were used as fitting parameters. In contrast to this, we determined the band offsets in a successive procedure from a coupling-induced shift and splitting of the optical transitions in a set of samples where the InAs layer thicknesses are the same and the exciton binding energies are known.

VI. CONCLUSIONS

In conclusion, we have determined the band offsets and the band-offset ratio at a highly strained InAs/GaAs interface by means of a method which employs the coupling between two identical ultrathin InAs layers separated by a GaAs barrier of different width, and exploits the large difference in electron and heavy-hole effective masses. With the InAs layer thickness (1.1 ML) and barrier widths (4, 8, 16, and 32 ML) known from x-ray-diffraction measurements, the band offsets could be extracted independently from the coupling-induced shift and splitting of the symmetric and antisymmetric hh- and lh-exciton transitions observed in PL and PLE. For that purpose, we introduced the δ-function potential for a description of the electronic structure of ultrathin InAs layers embedded in a GaAs matrix. In this approach it is inherently considered that no envelope function can be constructed within an InAs monolayer. As a consequence, the δ-potential provides only single bound electron hh and lh states, with their effective masses naturally being fixed to the values of the GaAs barrier in the direction of quantization. Applying our method, we find a conduction-band offset of $\Delta E_c = 535\,\mathrm{meV}$, a band-offset ratio of $Q_c = 0.58$, and a strain-induced splitting between the hh and lh subbands of $\delta E_{\text{hh-lh}} = 160\,\mathrm{meV}$. These results are in agreement with elasticity theory, and allow a satisfying description of the transition energies in ultrathin InAs layers as a function of InAs layer

thickness. Finally, we find that the lh confinement has been underestimated so far. With our lh band offset of $\Delta E_{\mathrm{lh}} = 225\,\mathrm{meV}$, the effective lh confinement energy amounts to 3 meV, which is about ten times larger than reported earlier. However, our value matches with the observation that the lh exciton remains bound at temperatures up to 18 K.

ACKNOWLEDGMENTS

This work was part of the research program of the Dutch Foundation for Fundamental Research on Matter (FOM), which is financially supported by the Dutch Organization for Advancement of Research (NWO).

*Present address: ASM Lithography, De Run 1110, 5503 LA Veldhoven, The Netherlands.

[1] T. Y. Wang and G. B. Springfellow, J. Appl. Phys. **67**, 344 (1990).
[2] E. P. O'Reilly, Semicond. Sci. Technol. **4**, 121 (1989).
[3] O. Brandt, L. Tapfer, R. Cingolani, K. Ploog, M. Hohenstein, and F. Phillipp, Phys. Rev. B **41**, 12 599 (1990).
[4] M. I. Alonso, M. Ilg, and K. Ploog, Phys. Rev. B **50**, 1628 (1994).
[5] O. Brandt, H. Lage, and K. Ploog, Phys. Rev. B **45**, 4217 (1992).
[6] P. D. Wang, N. N. Ledentsov, C. M. Sotomayor-Torres, I. N. Yassievich, A. Pakhomov, A. Yu. Egovov, P. S. Kop'ev, and V. M. Ustinov, Phys. Rev. B **50**, 1604 (1994).
[7] S. P. Kowalczyk, W. J. Schaffer, E. A. Kraut, and R. W. Grant, J. Vac. Sci. Technol. **20**, 705 (1982).
[8] C. Priester, G. Allan, and M. Lannoo, Phys. Rev. B **38**, 9870 (1988).
[9] C. G. van der Walle, Phys. Rev. B **39**, 1871 (1989).
[10] A. Sasaki, J. Cryst. Growth **160**, 27 (1996).
[11] H. Kitabayashi and T. Waho, J. Cryst. Growth **150**, 152 (1995).
[12] R. Cingolani, O. Brandt, L. Tapfer, G. Scamarcio, G. C. LaRocca, and K. Ploog, Phys. Rev. B **42**, 3209 (1990).
[13] S. L. Chuang, Phys. Rev. B **43**, 9649 (1991).
[14] F. H. Pollak, in *Effects of Homogeneous Strain on the Electronic and Vibrational Levels in Semiconductors*, edited by T. P. Pearsall, Semiconductors and Semimetals Vol. 32 (Academic, New York, 1990), p. 17.
[15] M. Nakayama, T. Fujita, I. Tanaka, H. Nishimura, and H. Terauchi, Jpn. J. Appl. Phys. **32**, 160 (1993).
[16] K. Taira, H. Kawai, I. Hase, K. Kaneko, and N. Watanabe, Appl. Phys. Lett. **53**, 495 (1988).
[17] J. Meléndez, A. Mazuelas, P. S. Dominguez, M. Garriaga, M. I. Alonso, G. Armelles, L. Tapfer, and F. Briones, Appl. Phys. Lett. **62**, 1000 (1993).
[18] O. Brandt, R. Cingolani, H. Lage, G. Scamarcio, L. Tapfer, and K. Ploog, Phys. Rev. B **42**, 11 396 (1990).
[19] I. Yassievich and U. Rössler, J. Phys. C **32**, 7927 (1994).
[20] R. P. Leavitt and J. W. Little, Phys. Rev. B **42**, 11 774 (1990).
[21] K. J. Moore, P. Dawson, and C. T. Foxon, Phys. Rev. B **38**, 3368 (1988).
[22] M. Sato and Y. Horikoshi, J. Appl. Phys. **66**, 851 (1989).
[23] S. S. Dosanjh, L. Hart, R. Nayak, and B. A. Joyce, J. Appl. Phys. **75**, 8066 (1994).
[24] M. G. Burt, Appl. Phys. Lett. **65**, 717 (1994).
[25] M. G. Burt, Phys. Rev. B **50**, 7518 (1994).
[26] A. Baldereshi and J. J. Hopfield, Phys. Rev. Lett. **28**, 171 (1972).
[27] H. P. Hjalmarsn, P. Vogl, D. J. Wolford, and J. D. Dow, Phys. Rev. Lett. **44**, 810 (1980).
[28] K. A. Mäder and Alfonso Baldereschi, Inst. Phys. Conf. Ser. **123**, 341 (1991).
[29] S. Wilke and D. Hennig, Phys. Rev. B **43**, 12 470 (1991).
[30] J. M. Luttinger, Phys. Rev. **102**, 1030 (1956).
[31] A. Yu. Silov, J. E. M. Haverkort, N. S. Averkiev, P. M. Koenraad, and J. H. Wolter, Phys. Rev. B **50**, 4509 (1994).
[32] P. D. Wang, N. N. Ledentsov, C. M. Sotomayor-Torres, P. S. Kop'ev, and V. M. Ustinov, Appl. Phys. Lett. **64**, 1526 (1994).
[33] N. N. Ledentsov, P. D. Wang, C. M. Sotomayor-Torres, A. Yu. Egorov, M. V. Maximov, V. M. Ustinov, A. E. Zhukov, and P. S. Kop'ev, Phys. Rev. B **50**, 12 171 (1994).
[34] S. S. Dosanjh, P. Dawson, M. R. Fahy, B. A. Joyce, R. A. Stradling, and R. Murray, J. Cryst. Growth **127**, 579 (1993).
[35] C. Giannini, L. Tapfer, S. Lagomarsino, J. C. Boulliard, A. Taccoen, B. Capelle, M. Ilg, O. Brandt, and K. Ploog, Phys. Rev. B **48**, 11 496 (1993).
[36] J. C. Woicik, J. G. Pellegrino, S. H. Southworth, P. S. Shaw, B. A. Karlin, and C. E. Bouldin, Phys. Rev. B **52**, R2281 (1995).
[37] T. Shima, J. S. Lee, K. Undo, K. Tanaka, S. Niki, A. Yamada, and Y. Makita, Appl. Surf. Sci. **75**, 164 (1994).
[38] F. Dujardin, N. Marréaud, and J. P. Laurenti, Solid State Commun. **98**, 297 (1996).
[39] J. Brübach, J. E. M. Haverkort, J. H. Wolter, P. D. Wang, N. N. Ledentsov, C. M. Sotomayor Torres, A. E. Zhukov, P. S. Kop'ev, and V. M. Ustinov, J. Opt. Soc. Am. B **73**, 1224 (1996).
[40] J. M. Gerard and J. Y. Marzin, Appl. Phys. Lett. **53**, 568 (1988).